Title

Magnetic resonance elastography predicts advanced fibrosis in patients with nonalcoholic fatty liver disease: a prospective study.

Journal

Hepatology (Baltimore, Md.), 60(6)

ISSN

0270-9139

Authors

Loomba, Rohit
Wolfson, Tanya
Ang, Brandon
et al.

Publication Date

2014-12-01

DOI

10.1002/hep.27362

Peer reviewed

HEPATOLOGY
Official Journal of the American Association for the Study of Liver Diseases

Magnetic Resonance Elastography Predicts Advanced Fibrosis in Patients With Nonalcoholic Fatty Liver Disease: A Prospective Study

Rohit Loomba,[1,2,3]* Tanya Wolfson,[4] Brandon Ang,[2] Jonathan Hooker,[8]** Cynthia Behling,[6] Michael Peterson,[5] Mark Valasek,[5] Grace Lin,[5] David Brenner,[1] Anthony Gamst,[4] Richard Ehman,[7] and Claude Sirlin[8]*

Retrospective studies have shown that two-dimensional magnetic resonance elastography (2D-MRE), a novel MR method for assessment of liver stiffness, correlates with advanced fibrosis in patients with nonalcoholic fatty liver disease (NAFLD). Prospective data on diagnostic accuracy of 2D-MRE in the detection of advanced fibrosis in NAFLD are needed. The aim of this study is to prospectively assess the diagnostic accuracy of 2D-MRE, a noninvasive imaging biomarker, in predicting advanced fibrosis (stage 3 or 4) in well-characterized patients with biopsy-proven NAFLD. This is a cross-sectional analysis of a prospective study including 117 consecutive patients (56% women) with biopsy-proven NAFLD who underwent a standardized research visit: history, exam, liver biopsy assessment (using the nonalcoholic steatohepatitis Clinical Research Network histological scoring system), and 2D-MRE from 2011 to 2013. The radiologist and pathologist were blinded to clinical and pathology/imaging data, respectively. Receiver operating characteristics (ROCs) were examined to assess the diagnostic test performance of 2D-MRE in predicting advanced fibrosis. The mean (± standard deviation) of age and body mass index was 50.1 (± 13.4) years and 32.4 (± 5.0) kg/m^2, respectively. The median time interval between biopsy and 2D-MRE was 45 days (interquartile range: 50 days). The number of patients with fibrosis stages 0, 1, 2, 3, and 4 was 43, 39, 13, 12, and 10, respectively. The area under the ROC curve for 2D-MRE discriminating advanced fibrosis (stage 3-4) from stage 0-2 fibrosis was 0.924 ($P < 0.0001$). A threshold of >3.63 kPa had a sensitivity of 0.86 (95% confidence interval [CI]: 0.65-0.97), specificity of 0.91 (95% CI: 0.83-0.96), positive predictive value of 0.68 (95% CI: 0.48-0.84), and negative predictive value of 0.97 (95% CI: 0.91-0.99). *Conclusions:* MRE is accurate in predicting advanced fibrosis and may be utilized for noninvasive diagnosis of advanced fibrosis in patients with NAFLD. (HEPATOLOGY 2014;60:1920-1928)

Nonalcoholic fatty liver disease (NAFLD) is characterized by the presence of hepatic steatosis in individuals who consume little or no alcohol and who have no other identifiable secondary cause of steatosis.[1-5]. NAFLD is associated with features of metabolic syndrome, including obesity, insulin resistance, hypertension, diabetes, and dyslipidemia.[1,4,6,7] It is the most common cause of chronic liver disease (CLD) in the United States.[2-5] It affects 80-100 million Americans, of whom 10%-22% may have nonalcoholic steatohepatitis (NASH),[8-13] a progressive form that may lead to cirrhosis[11, 14] and

Abbreviations: 2D, two-dimensional; AIC, Akaike Information Criterion; ALP, alkaline phosphatase; ALT, alanine aminotransferase; AST, aspartate aminotransferase; AUROC, area under the ROC curve; BMI, body mass index; BW, bandwidth; CI, confidence interval; CLD, chronic liver diseases; FA, flip angle; FFAs, free fatty acids; FOV, field of view; GGT, gamma-glutamyl transferase; HbA1C, hemoglobin A1C; kPa, kilopascals; MR, magnetic resonance; MRE, magnetic resonance elastography; MRI, magnetic resonance imaging; NAFLD, nonalcoholic fatty liver disease; NASH, nonalcoholic steatohepatitis; NASH-CRN, NASH Clinical Research Network; NPV, negative predictive value; PDFF, proton density fat fraction; PPV, positive predictive value; ROC, receiver operating characteristic; ROIs, regions of interest; SD, standard deviation; TE, echo time; TG, triglyceride; TR, repetition time; UCSD, University of California at San Diego.

From the [1]Division of Gastroenterology and [2]NAFLD Translational Research Unit, Department of Medicine, and [3]Division of Epidemiology, Department of Family and Preventive Medicine, University of California at San Diego, La Jolla, CA; Departments of [4]Mathematics and [5]Pathology, University of California at San Diego, La Jolla, CA; [6]Department of Pathology, Sharp Health System, San Diego,, CA; [7]Department of Radiology, Mayo Clinic, Rochester, MN; and [8]Liver Imaging Group, Department of Radiology, University of California at San Diego, La Jolla, CA.

Received January 31, 2014; accepted July 30, 2014.

Additional Supporting Information may be found at onlinelibrary.wiley.com/doi/10.1002/hep.27362/suppinfo.

hepatocellular carcinoma.[11,15-19] Patients with NASH and especially those with advanced fibrosis are at particularly high risk for these outcomes and require more-intense monitoring and therapy. The current diagnostic gold standard to diagnose advanced fibrosis is liver biopsy.[20] However, biopsy is invasive and costly and may be complicated by morbidity and even death.[21] Accurate noninvasive objective methods to detect advanced fibrosis in patients with NAFLD are needed, but are not yet commercially available.

There are no approved noninvasive tests to diagnose advanced fibrosis. Cytokeratin-18,[22] NAFLD fibrosis score,[23] and Enhanced Liver Fibrosis (ELF^{TM}) Test[24] are promising, but may not be sufficiently accurate for routine clinical use.[1, 25] Ultrasound elastography methods have high (21%-50%) failure rates in NAFLD.[26-29] Recent retrospective studies demonstrate that two-dimensional magnetic resonance (MR) elastography (2D-MRE) may be useful in noninvasive diagnosis of advanced fibrosis in NAFLD.[30] However, prospective studies of 2D-MRE with paired liver biopsies in well-characterized patients with biopsy-proven NAFLD with a clinical indication for a liver biopsy are needed.

Utilizing a prospective cohort study design, we aimed to determine the accuracy of 2D-MRE for noninvasive diagnosis of advanced fibrosis in well-characterized patients with biopsy-proven NAFLD. We also aimed to determine the accuracy of 2D-MRE for noninvasive diagnosis of the presence of NASH, as well as dichotomized stages of fibrosis.

Patients and Methods

Design. This is a cross-sectional analysis of a prospective cohort study including 117 consecutive patients with biopsy-proven NAFLD who also underwent an advanced MR examination, including 2D-MRE. All patients had a histology-confirmed diagnosis of NAFLD. Liver biopsies were performed for clinical care, and 2D-MRE was done for research. After careful exclusion of other causes of liver diseases and secondary causes of hepatic steatosis, patients attended a research clinic visit and underwent standardized history, physical exam, anthropometric exam, and biochemical testing at the University of California at San Diego (UCSD) NAFLD Translational Research Unit[31-33] and a 2D-MRE examination at the UCSD MR3T Research Laboratory. All patients provided written informed consent, and the study was approved by the UCSD Institutional Review Board as well as the UCSD Clinical and Translational Research Institute.

Patient Population. Patients were included if they met the following inclusion and exclusion criteria.

Inclusion/Exclusion Criteria. Patients were included if they were $\geq$18 years of age, had a liver biopsy confirming NAFLD, and provided written informed consent. Exclusion criteria were regular and excessive alcohol consumption within 2 years preceding recruitment: $\geq$14 (men) or $\geq$7 (women) drinks per week, use of hepatotoxic drugs or drugs known to cause hepatic steatosis, clinical or laboratory evidence of secondary NAFLD resulting from major nutritional and iatrogenic gastrointestinal disorders or to human immunodeficiency virus infection, clinical or laboratory evidence of liver disease other than NAFLD, such as viral hepatitis (shown by a positive serum hepatitis B surface antigen or hepatitis C viral RNA), Wilson's disease, hemochromatosis, glycogen storage disease, alpha 1-antitrypsin deficiency, autoimmune hepatitis, cholestatic or vascular liver disease, clinical or biochemical evidence of decompensated liver disease with

The study was conducted at the Clinical and Translational Research Institute, University of California at San Diego. R.L. is supported, in part, by the American Gastroenterological Association (AGA) Foundation (Sucampo) ASP Designated Research Award in Geriatric Gastroenterology and by a T. Franklin Williams Scholarship Award; funding provided by: Atlantic Philanthropies, Inc; the John A. Hartford Foundation, the Association of Specialty Professors, and the American Gastroenterological Association and grant K23-DK090303. Additional funding provided by R01DK088925 (principal investigator [PI]: C.S.) and National Institutes of Health grant EB001981 (PI: R.E.).

The study sponsor(s) had no role in the study design, collection, analysis, interpretation of the data, and/or drafting of the manuscript.

**These authors contributed equally to this work.*

***Correction added after publication October 29, 2014: Author name Jonathan Booker was changed to Jonathan Hooker.*

Address reprint requests to: Rohit Loomba, M.D., M.H.Sc., Division of Gastroenterology and Epidemiology, University of California at San Diego, 9500 Gilman Drive, MC 0063, La Jolla, CA 92093. E-mail: roloomba@ucsd.edu; fax: +1-858-534-3338 or Claude Sirlin, M.D., Liver Imaging Group, Department of Radiology, University of California at San Diego, 408 Dickinson Street, San Diego, CA 92103-8226. E-mail: csirlin@ucsd.edu; Fax: +1-619-471-0503.

View this article online at wileyonlinelibrary.com.

DOI 10.1002/hep.27362

Potential conflict of interest: Dr. Ehman owns stock in, holds intellectual property rights to, and received grants from Resoundant, Inc. Dr. Sirlin consults, advises, and is on the speakers' bureau for Bayer. He received grants from GE Healthcare.

Child-Pugh score greater than 7 points, active substance abuse or significant systemic illnesses, contraindication(s) to magnetic resonance imaging (MRI), pregnant or trying to become pregnant, or any condition that, in an investigator's opinion, impedes participant competence, compliance, or study completion.

Histologic Assessment. All patients underwent a systematic liver biopsy evaluation that was scored using the nonalcoholic steatohepatitis (NASH) Clinical Research Network (NASH-CRN) histological scoring system.[34] Each biopsy was read in a blinded fashion by an experienced liver pathologist without knowledge of clinical and radiology data.

Liver fibrosis stage was scored on a 5-point ordinal scale (0, 1, 2, 3, and 4). Patients with stage 3 (bridging fibrosis) and stage 4 (cirrhosis) were classified as having advanced fibrosis.NASH was scored on a 3-point ordinal scale (non-NASH, borderline NASH, and definite NASH). For the purpose of this study, patients with borderline as well as definite NASH were classified as having NASH. The average (± standard deviation [SD]) of biopsy size and number of portal triads were 23.8 (± 9.6) mm and 13.7 (± 5.9), respectively.

Outcome Measures. Primary outcome was advanced fibrosis: All patients with liver biopsy evidence of stage 3 (bridging fibrosis) or stage 4 (cirrhosis) were classified as having advanced fibrosis. Secondary outcomes included (1) NASH and (2) dichotomized fibrosis stages, including stage 0 versus stage 1-4, stage 0-1 versus stage 2-4, and stage 0-3 versus stage 4.

MRI. MRI examinations were performed using a 3T research scanner (GE Signa EXCITE HDxt; GE Healthcare, Waukesha, WI) at the UCSD MR3T Research Laboratory. Patients were scanned in the supine position with a torso phased array coil placed over the abdomen. To reduce potential physiological confounding factors, patients were instructed to fast a minimum of 4 hours. The duration of fasting was not recorded. Two MR techniques were performed: 2D-MRE, to estimate liver stiffness, and an advanced MR fat quantification technique.

2D-MRE. MRE was performed as previously described,[35-38] using commercially available software and hardware (Resoundant Inc., Rochester, MN). Briefly, an acoustic passive driver is secured with an elastic band over the body wall anterior to the liver and connected by a flexible plastic tube to an acoustic active driver outside the MRI room. Continuous vibrations at 60 Hz are generated by the active driver and delivered by the tube to the passive driver, which then transmits the vibrations into the body, thereby producing shear waves in the liver. A 2D gradient-recalled/echo MRE pulse sequence is performed while the vibrations are transmitted, and four noncontiguous axial slices (10-mm thick, 10-mm interslice gap) are acquired in a 16-second breath-hold through the widest transverse dimension of the liver. Acquisition parameters include the following: repetition time (TR), 50 ms; echo time (TE), 20.2 ms; flip angle (FA), 30 degrees; matrix, 256 × 64; field of view (FOV), 48 × 48 cm; one-signal average; receiver bandwidth (BW) ± 33 kHz (confirm); and parallel imaging acceleration factor, 2. By utilizing oscillating motion-sensitizing gradients that encode tissue motion into the phase of the MR signal, this sequence generates images (called wave images) that depict the shear waves within the liver. The sequence is repeated a total of four times, adjusting the phase relationship (phase offset) between the vibrations and the oscillating motion-sensitizing gradients, thereby producing, at each slice location, wave images at four evenly spaced time points over the wave cycle. Total acquisition time (four 16-second breath-holds with short recovery in between) is around 2 minutes.

The wave images at each slice location then are processed automatically on the scanner computer using specialized software (called an inversion algorithm) to generate quantitative cross-sectional maps (called elastograms) depicting the stiffness of tissue. Four elastograms are generated, one at each of the four slice locations. These maps display stiffness with a color scale in units of kilopascals (kPa).

The elastograms were transferred offline for analysis.[31,33] A trained image analyst (6 months of experience with MRE) in the MR3T research laboratory manually drew regions of interest (ROIs) on the elastograms using a custom software package. ROIs were drawn at each of the four slice locations in portions of the liver in which the corresponding wave images showed clearly observable wave propagation, avoiding liver edges, large blood vessels, and artifacts. The mean liver stiffness was calculated by averaging the per-pixel stiffness values across the ROIs at the four slice locations, and the results were outputted automatically to an electronic spreadsheet.

MRI/Proton Density Fat Fraction. To quantify liver fat content, we used an advanced fat quantification MR technique, as previously described.[32,39-41] Briefly, this 2D magnitude-based gradient-recalled/echo technique estimates proton density fat fraction (PDFF), an MRI-based biomarker of liver fat content,[40,42,43] using low FA (10 degrees), relative to TR (≥125 ms), to minimize T_1 bias[40,41,44] and six gradient-recalled echoes at sequential in- and out-of-phase TEs (1.15, 2.3, 3.45, 4.6, 5.75, and 6.9 ms) to separate fat and

water signals and calculate and correct for T_2^* signal decay.[40,41,44,45] 2D contiguous slices (10-mm thick, 0-mm interslice gap) are acquired of the entire liver in a single 18- to 30-second breath-hold. Other acquisition parameters include receiver BW ±142 kHz, base matrix 224 × 124, one-signal average, rectangular FOV adjusted to body habitus and breath-hold capacity, and a parallel imaging factor of 1.25. Cross-sectional maps depicting the PDFF of tissue are computed pixel-by-pixel from source images using custom-developed software that models observed signal as a function of TE, taking into account the multiple frequency components of triglyceride (TG).[41,44,46-48]

This technique has been shown to accurately quantify fat content in phantoms[44] and in human liver *in vivo* at both 1.5 and 3T using MR spectroscopy[40,41,49,50] with contemporaneous liver biopsy[33,39] as a reference. The technique has high intra- and inter-examination repeatability[40] and high reproducibility across field strength[49,50] and scanner manufacturer[50] and is robust to acquisition parameter variation over the clinically reasonable range.[49] MRI-estimated PDFF is more accurate than conventional dual-phase imaging[40,43] and, unlike conventional imaging, remains accurate even in the setting of iron overload,[45] which may coexist with NAFLD.

The PDFF maps were transferred offline for analysis. A trained image analyst (6 months of experience with MRE) in the MR3T research laboratory manually placed 2-cm-diameter circular ROIs in each of the nine hepatic segments on the maps, avoiding large blood vessels, liver edges, and (if any) artifacts.[39,51] The mean liver PDFF was calculated by averaging the per-pixel PDFF values across the ROIs in each segment, and the results were outputted automatically to an electronic spreadsheet.

Duration Between 2D-MRE and Liver Biopsy. The median time interval between biopsy and 2D-MRE was 45 days (interquartile range: 50 days).

Clinical Research Assessment. All patients were evaluated in the UCSD NAFLD Translational Unit research clinic. A detailed history was ascertained from all patients. A physical exam, including vital signs, height, weight, and anthropometric measurements, was performed by a trained investigator. Body mass index (BMI) was calculated by dividing body weight (in kilograms) by the square of the height (in meters). Alcohol consumption was documented in clinical visits and then confirmed in the research clinic using the Alcohol Use Disorders Identification Test and Skinner questionnaire, validated tools used to screen for heavy drinking and/or active alcohol abuse or dependence. A detailed history of medications was also obtained; none of the patients included in this study reported use of medications known or suspected to induce steatosis or steatohepatitis. Other causes of liver disease or injury were systematically ruled out in a standardized and uniform manner based on historical and laboratory data. Subjects underwent biochemical phenotyping, which consisted of alanine aminotransferase (ALT), aspartate aminotransferase (AST), alkaline phosphatase (ALP), gamma-glutamyl transpeptidase (GGT), total bilirubin, direct bilirubin, albumin, hemoglobin A1c (HbA1c), fasting glucose and insulin, homeostatic model assessment of insulin resistance, as defined by the product of glucose and insulin divided by 405, prothrombin time/international normalized ratio, fasting lipid panel, free fatty acids (FFAs), C-reactive protein, and platelet count.

Statistical Analyses. An experienced biostatistical analyst (T.W.) performed the statistical analyses under the supervision of a faculty statistician (A.G.) using "R" statistical computing software (R version 2.15.1 [2012-06-22]; R: a language and environment for statistical computing; R Foundation for Statistical Computing, Vienna, Austria). A two-tailed P value of ≤ 0.05 was considered statistically significant for all analyses.

Patients' demographic, laboratory, histological, and imaging data were summarized. Summary statistics are presented as mean and SD for continuous measures and as numbers and percentages for categorical measures.

Main Analysis and Cross-Validation. Receiver operating characteristic (ROC) curve analysis was performed for 2D-MRE as a classifier of advanced fibrosis (stage 3 or 4 fibrosis). The measure of overall performance was the area under the ROC curve (AUROC). The cut-off value of 2D-MRE for classifying advanced fibrosis was selected to optimize sensitivity with specificity at 90% or greater; for that cut-off value, the following performance parameters were computed: sensitivity; specificity; positive predictive value (PPV); negative predictive value (NPV); and total accuracy. Stratified 10-fold cross-validation was applied to the threshold selection method, and cross-validated performance parameters were computed. Ninety-five percent binomial confidence intervals (CIs) were computed around both raw and cross-validated performance parameters.

Secondary Analyses. Similarly, ROC analyses were performed and the corresponding AUROCs, classifying thresholds, performance parameters, and cross-validated performance parameters were computed for 2D-MRE as a classifier of NASH and other dichotomizations of fibrosis stage (any fibrosis [stage ≥ 1; stages 0-1 vs. 2-4

Table 1. Baseline Demographic, Biochemical, and Histological Characteristics of Subjects

Characteristic	Patients With Paired Biopsy and 2D-MRE (n = 117)
Demographics	
Male patients (%)	51 (43.6)
Age, years	50.1 (13.4)
Weight (kg), mean (SD)	91.8 (18.4)
Height (m), mean (SD)	1.68 (0.11)
BMI (kg/m^2), mean (SD)	32.4 (5.0)
Ethnic origin (%)	
White	61 (52.1)
Black	1 (0.9)
Asian	20 (17.1)
Hispanic	32 (27.4)
Multi-racial	1 (0.9)
Other	1 (0.9)
Refused to disclose	1 (0.9)
Diabetes (%)	40 (34.19)
Biochemical profile	
ALT (U/L), mean (SD)	66.3 (54.4)
AST (U/L), mean (SD)	45.4 (31.3)
AST/ALT ration, mean (SD)	0.77 (0.30)
ALP (U/L), mean (SD)	74.7 (23.4)
GGT (U/L), mean (SD)	59.3 (47.6)
Total bilirubin (mg/dL), mean (SD)	0.5 (0.4)
Direct bilirubin (mg/dL), mean (SD)	0.1 (0.08)
Albumin (g/dL), mean (SD)	4.5 (0.3)
Glucose (mg/dL), mean (SD)	107.1 (30.3)
HbA1C, mean (SD)	6.1 (0.9)
TG (mg/dL), mean (SD)	166.9 (98.7)
Total cholesterol (mg/dL), mean (SD)	186.0 (39.4)
LDL (mg/dL), mean (SD)	106.2 (34.2)
HDL (mg/dL), mean (SD)	48.4 (16.6)
Prothrombin time, mean (SD)	10.8 (1.0)
Histology	
Steatosis (%)	
1	41 (35.0)
2	43 (36.8)
3	33 (28.2)
Lobular inflammation (%)	
0	2 (1.7)
1	46 (39.3)
2	64 (54.7)
3	5 (4.3)
Ballooning (%)	
0	16 (13.7)
1	77 (65.8)
2	24 (20.5)
Fibrosis (%)	
0	43 (36.8)
1	39 (33.3)
2	13 (11.1)
3	12 (10.3)
4	10 (8.5)
NASH	
NAFLD, not NASH (%)	11 (9.4)
Borderline NASH (%)	15 (12.8)
Definite NASH (%)	91 (77.8)
NAS, mean (SD)	4.62 (1.36)
2D-MRE, mean (SD)	3.17 (1.19)

All labs were measured while fasting. The NASH CRN histological scoring system was used for histological grading and staging of liver biopsy.

Abbreviations: LDL, low-density lipoprotein; HDL, high-density lipoprotein; NAS, NAFLD Activity Score.

and stages 0-3 vs. 4). Finally, we used multivariable logistic regression to explore the contribution of additional predictors of the primary outcome of advanced fibrosis, including age, sex, BMI, and MRI-PDFF. The Akaike Information Criterion (AIC) was used to select the model with the optimal combination of predictors.

Results

Baseline Characteristics. Between January 2011 and November 2013, 117 consecutive patients (56% women) with biopsy-proven NAFLD and paired 2D-MRE were prospectively enrolled in this MRE study. The mean (± SD) of age and BMI was 50.07 (± 13.4) years and 32.42 (± 5) kg/m^2, respectively. Baseline characteristics, including demographics, biochemical, histological, and imaging data, are presented in Table 1.

A total of 164 patients were observed in the NAFLD Translational Unit, and 47 of these did not undergo MRE. Supporting Table 1 describes the baseline characteristics of patients who underwent MRE (n = 117) versus those who did not undergo MRE (n = 47). Compared to patients who had an MRE, those who did not have an MRE were more likely to have milder disease and less likely to have NASH and features of advanced disease on biopsy.

Distribution of Fibrosis Stage. The number of patients with fibrosis stages 0, 1, 2, 3, and 4 were 43, 39, 13, 12, and 10, respectively. The prevalence of advanced fibrosis (stage 3 or 4) was 19% (22 of 117).

Accuracy of 2D-MRE in the Diagnosis of Advanced Fibrosis. The AUROC for MRE discriminating advanced fibrosis from stage 0-2 fibrosis was 0.924 ($P < 0.0001$), as shown in Fig. 1. The best threshold of >3.64 kPa had a raw sensitivity of 0.86 (95% CI: 0.65-0.97), specificity of 0.91 (95% CI: 0.83-0.96), PPV of 0.68 (95% CI: 0.48-0.84), and NPV of 0.97 (95% CI: 0.91-0.99), as shown in Table 2. A box plot of individual stages of fibrosis (stages 0, 1, 2, 3, and 4) shown on the x-axis and the respective 2D-MRE reading on the y-axis is shown for the entire cohort stratified by fibrosis stage (Fig. 2). MRE images of 5 representative patients with stage 0, 1, 2, 3, and 4 fibrosis are shown in Fig. 3. Twelve patients were misclassified. Nine patients with stage 0-2 fibrosis on biopsy were classified as having advanced fibrosis, and 3 with stage 3-4 fibrosis were classified as having stage 0-2 fibrosis. Cross-validation of the method yielded a sensitivity 0.86 (95% CI: 0.58-0.95), specificity of 0.91 (95% CI: 0.84-0.96), PPV of 0.67 (95% CI: 0.44-0.83), and NPV of 0.97 (95% CI: 0.90-0.99).

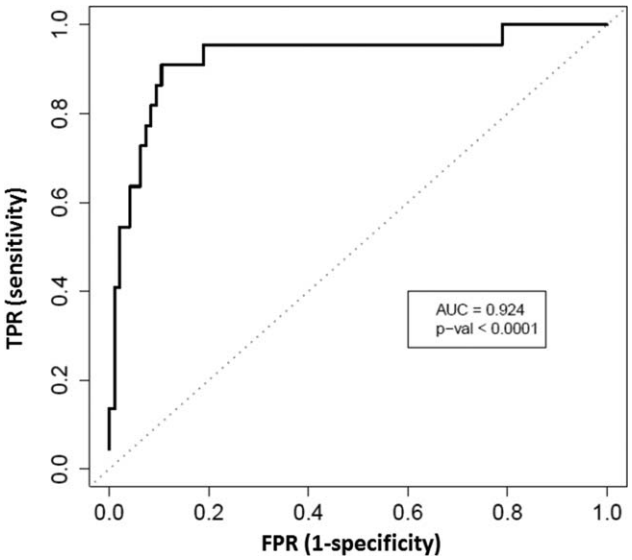

Fig. 1. Diagnostic accuracy of MRE for advanced fibrosis. AUROC for the detection of advanced fibrosis in patients with biopsy-proven NAFLD is shown, and a two-tailed *P* value is provided. TPR, true-positive rate; FPR, false-positive rate.

Multivariable-Adjusted Model. Step-wise logistic regression with AIC as a selection criterion was used to identify a model with the optimal combination of predictors of advanced fibrosis, choosing from 2D-MRE, MRI-PDFF, age, sex, and BMI. Addition of liver fat content using MRI-PDFF as a variable did not improve the AUROC, suggesting that liver fat content did not change the prediction for advanced fibrosis by 2D-MRE. Therefore, MRI-PDFF was not included in further models. Furthermore, sex was dropped as a predictive variable in the optimal AIC determined prediction model. Thus, the final model contained 2D-MRE plus age and BMI as predictors. The AUROC for classifying advanced fibrosis based on the fitted variable (a weighted combination of predictors including 2D-MRE, age, and BMI) from the multivariable model was 0.95 ($P < 0.001$; see Supporting Fig. 1). However, the performance in classifying advanced fibrosis (both raw and cross-validated) was similar to that of the univariate (2D-MRE based only) model, with a slight gain in specificity and total classification accuracy and a slight loss in sensitivity.

Presence of NASH and Dichotomized Fibrosis Stages. Table 2 provides the details of the diagnostic test characteristics of 2D-MRE for the diagnosis of NASH, as well as various dichotomized stage of fibrosis. The AUROC for diagnosis of NASH was 0.73 ($P < 0.0001$). The AUROC for discriminating stage 0 versus stage 1-4 was 0.84 ($P < 0.0001$), for stage 0-1 versus stage 2-4 was 0.86 ($P < 0.0001$), and for stage 0-3 versus stage 4 was 0.89 ($P < 0.0001$).

Discussion

Main Findings. Utilizing a prospective cohort study design, our study demonstrated that 2D-MRE accurately detects advanced fibrosis in patients with biopsy-proven NAFLD. In addition, we showed that 2D-MRE accurately detects cirrhosis. These data have important clinical implications, given that noninvasive diagnosis of advanced fibrosis is a major unmet need in the field, and 2D-MRE can be reliably utilized to noninvasively screen (rule out) advanced fibrosis in patients with NAFLD. This study provides prospective validation to previously conducted retrospective studies. With a rising interest in antifibrotic therapies in NAFLD, 2D-MRE would also be helpful for screening for antifibrotic clinical trials that are specifically targeting patients with advanced fibrosis (stage 3 or 4). Therefore, we propose that 2D-MRE is an accurate, noninvasive imaging-based biomarker, which may be utilized for diagnosis of advanced fibrosis and cirrhosis in patients with NAFLD.

In Context With Published Literature. Our findings are in agreement with previous retrospective studies in a mixed population of patients with various etiologies

Table 2. Diagnostic Test Characteristics of 2D-MRE in the Detection of Advanced Fibrosis as Well as Other Secondary Outcomes

	N Positive	N Negative	AUC	Cutoff (Kpa)	Raw Sensitivity	Raw Specificity	Raw PPV	Raw NPV	CV Sensitivity	CV Specificity	CV PPV	CV NPV
Primary												
Stage 0, 1, 2 vs. 3, 4	22	95	0.924	**3.64**	0.864	0.905	0.679	0.966	0.818	0.895	0.643	0.955
Secondary												
Stage 0 vs. 1, 2, 3, 4	74	43	0.838	**3.02**	0.554	0.907	0.911	0.542	0.446	0.907	0.892	0.488
Stage 0, 1 vs. 2, 3, 4	35	82	0.856	**3.58**	0.657	0.915	0.767	0.862	0.629	0.915	0.759	0.852
Stage 0, 1, 2, 3 vs. 4	10	107	0.894	**4.67**	0.8	0.944	0.571	0.981	0.7	0.925	0.467	0.971
No NASH vs. NASH	91	26	0.733	**3.26**	0.42	0.923	0.951	0.316	0.429	0.885	0.929	0.307
Multivariable-adjusted stage 0, 1, 2 vs. 3, 4	22	95	0.952	**3.64**	0.864	0.905	0.679	0.966	0.818	0.905	0.667	0.956

Multivariable-adjusted model includes age and sex adjustment.

Abbreviations: N, number of patients; AUC, area under the curve; CV, cross-validated.

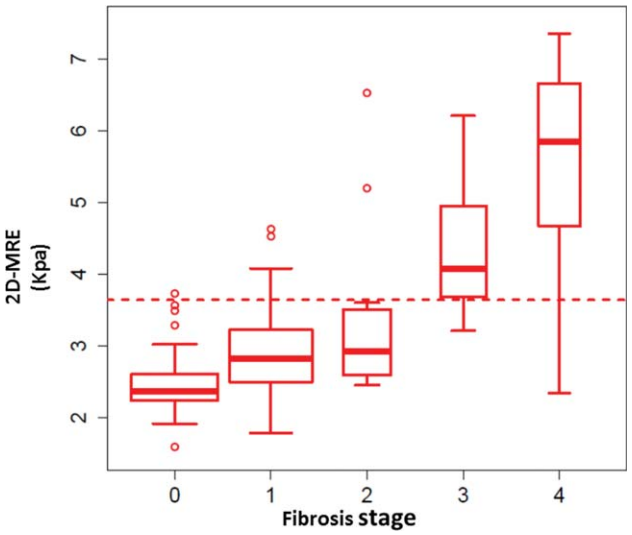

Fig. 2. Distribution of fibrosis and MRE readings for the entire cohort. A box plot of individual stages of fibrosis (stage 0, 1, 2, 3, and 4) is shown on the x-axis, and the respective 2D-MRE reading on the y-axis is shown for the entire cohort stratified by fibrosis stage.

of CLDs in assessing the diagnostic accuracy of 2D-MRE in the detection of advanced fibrosis.[35,52] Yin et al. had previously shown that liver fat content, as estimated using a conventional in- and out-of-phase imaging technique, did not affect the 2D-MRE assessment of hepatic fibrosis in a retrospective study of a cohort with a variety of CLDs.[35] We confirmed their findings prospectively in a NAFLD cohort using a more advanced, accurate, and standardized fat quantification technique.[31-33] Furthermore, we showed that addition of age and BMI (simple routinely available variables to either radiologists or patients themselves without the need of any invasive blood draw) further improved the diagnostic accuracy of 2D-MRE in detection of advanced fibrosis, but there was only a slight improvement in the number of patients who were correctly classified. In another recent retrospective study, Kim et al. showed that 2D-MRE was accurate in the diagnosis of advanced fibrosis in NAFLD.[30] Our study is a prospective validation of previous retrospective studies. Furthermore, this is the first prospective study to evaluate 2D-MRE in consecutive patients with biopsy-proven NAFLD for other dichotomized fibrosis stages. Although we found similarly high accuracy for the diagnosis of advanced fibrosis, the diagnostic accuracy of 2D-MRE for detection of NASH in this prospective study was lower than previously reported in a retrospective study by Chen et al.[36] We utilized the well-established NASH-CRN histological scoring system for assessment of NASH in this study, whereas Chen et al. classified patients by presence of inflammation (yes/no) and fibrosis (yes/no), rather than a standard definition of NASH, which may explain the discrepancy. Liver biopsy is considered a gold standard for assessment of fibrosis stage, but it clearly does not accurately classify all patients correctly into an individual fibrosis stage. Hence, when the gold standard is imperfect, even a test (hypothetical scenario) that has an accuracy of 100% may not always yield an AUROC >0.95, given the inherent limitations of the liver biopsy assessment. MRE readings may be inaccurate in certain conditions, such as acute inflammation and iron overload, and therefore the test has to be utilized in the appropriate clinical context. Based upon previous studies and expert panel reviews, transient elastography is useful in assessing advanced fibrosis, but has a high failure rate as well as a high rate of unreliable values (approximately 21%-50%), particularly in patients with NAFLD because of higher prevalence of obesity in this patient population.[1,26-29,53,54] Among available prediction rules, NAFLD fibrosis score provides a clinically useful model for screening for advanced fibrosis in patients with NAFLD.[23] However, more-accurate tests are desirable. Several serum- and plasma-based biomarkers have been assessed for the diagnosis of advanced fibrosis, but none of them are ready for routine clinical use because of high misclassification rates.[1,55] 2D-MRE

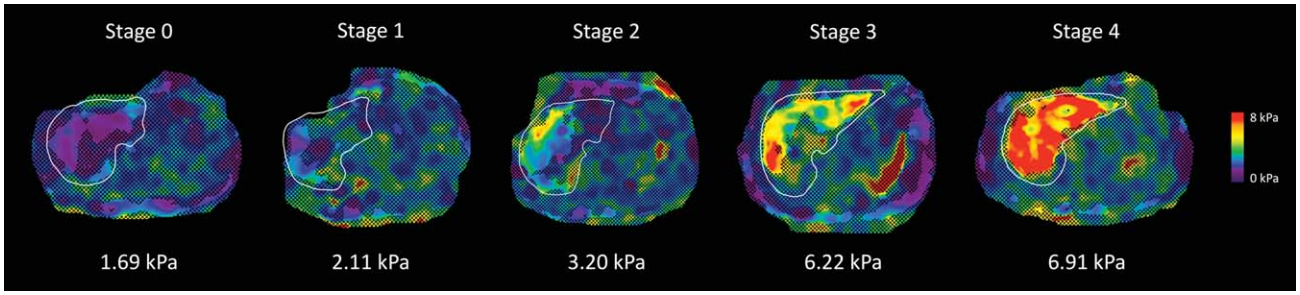

Fig. 3. MRE stiffness maps of 5 patients with NAFLD and different stages of liver fibrosis. Shown are MRE stiffness maps in 5 patients with NAFLD. These maps depict the spatial distribution of stiffness (in kPa) within the liver (outlined in white). As shown in the color lookup table at the right, the stiffness values range from near zero (dark purple) to 8 kPa (red). The histology-determined liver fibrosis stage is shown at the top of each stiffness map, and the MRE-determined mean liver stiffness is shown at the bottom of each image. Notice that the stiffness values are greater in patients with more-advanced fibrosis.

is promising and emerging to be an accurate tool for assessing advanced fibrosis and risk of decompensation, but requires independent validation in a prospective, multicenter study.[30,56]

Strengths and Limitations. The key novelty and innovation of the study lies in the prospective nature of the study, and the utilization of a well-characterized cohort of patients with biopsy-proven NAFLD, each of whom had a clinical indication for liver biopsy. Advanced MRI techniques (2D-MRE and MRI-PDFF estimation) were conducted by an experienced group of investigators, and the median time interval between the MR examinations and biopsy was 45 days. Liver biopsy examination was used as the gold standard for assessment of fibrosis using the NASH-CRN histological scoring system. All patients underwent a dedicated research visit, and other causes of liver disease were excluded. The diagnosis of NAFLD was systematically ascertained, and the study was conducted in a dedicated NAFLD translational research unit. However, we would like to acknowledge the following limitations of this study. This is a single-center study conducted at a specialized center for both clinical and MRI research in NAFLD, suggesting strong internal validity, but generalizability remains to be determined in a multicenter setting. This is a cross-sectional study, and these data do not provide evidence regarding longitudinal utility of 2D-MRE in assessment of changes in liver fibrosis. MRI-based methods may be expensive, but, at our center, the cost of MRE is less than that of a liver biopsy. However, clinical MRI plus MRE fees may be cost prohibitive at certain sites. Further studies are needed to assess cost-effectiveness of using MRE over other available modalities for the diagnosis of advanced fibrosis in patients with NAFLD. Significant refinement in technology and faster acquisition of 2D-MRE data is underway that may further reduce cost.

Impact on Clinical Practice and Future Directions. This study provides prospective data on the diagnostic accuracy of 2D-MRE in patients with biopsy-proven NAFLD. These data suggest that 2D-MRE has excellent accuracy in determining advanced fibrosis in patients with NAFLD and confirms previously conducted retrospective studies. Based upon evidence derived from previously conducted retrospective studies, and this prospective study, 2D-MRE may be utilized for noninvasive detection of advanced fibrosis in patients with NAFLD. In contrast to previous retrospective studies, we found that the performance of 2D-MRE for diagnosis of NASH versus NAFL was rather modest and did not provide a high level of accuracy. Further prospective and multicenter studies are needed to assess the role of 2D-MRE in assessing longitudinal changes in monitoring liver fibrosis and disease progression in the setting of both natural history studies as well as intervention trials. Further prospective studies are also needed to assess the role of novel MRE parameters, and more-advanced MRE methods (such as 3D-MRE) in the noninvasive diagnosis of NASH, and fibrosis in well-characterized patients with biopsy-proven NAFLD.

References

1. Chalasani N, Younossi Z, Lavine JE, Diehl AM, Brunt EM, Cusi K, et al. The diagnosis and management of non-alcoholic fatty liver disease: practice Guideline by the American Association for the Study of Liver Diseases, American College of Gastroenterology, and the American Gastroenterological Association. Hepatology 2012;55:2005-2023.
2. Targher G, Day CP, Bonora E. Risk of cardiovascular disease in patients with nonalcoholic fatty liver disease. N Engl J Med 2010;363: 1341-1350.
3. Williams CD, Stengel J, Asike MI, Torres DM, Shaw J, Contreras M, et al. Prevalence of nonalcoholic fatty liver disease and nonalcoholic steatohepatitis among a largely middle-aged population utilizing ultrasound and liver biopsy: a prospective study. Gastroenterology 2011;140:124-131.
4. Loomba R, Abraham M, Unalp A, Wilson L, Lavine J, Doo E, Bass NM; Nonalcoholic Steatohepatitis Clinical Research Network. Association between diabetes, family history of diabetes, and risk of nonalcoholic steatohepatitis and fibrosis. Hepatology 2012;56:943-951.
5. Welsh JA, Karpen S, Vos MB. Increasing prevalence of nonalcoholic fatty liver disease among United States adolescents, 1988-1994 to 2007-2010. J Pediatr 2013;162:496-500.e1.
6. Zarrinpar A, Loomba R. Review article: the emerging interplay among the gastrointestinal tract, bile acids and incretins in the pathogenesis of diabetes and non-alcoholic fatty liver disease. Aliment Pharmacol Ther 2012;36:909-921.
7. Loomba R, Sanyal AJ. The global NAFLD epidemic. Nat Rev Gastroenterol Hepatol 2013;10:686-690.
8. Browning JD, Szczepaniak LS, Dobbins R, Nuremberg P, Horton JD, Cohen JC, et al. Prevalence of hepatic steatosis in an urban population in the United States: impact of ethnicity. Hepatology 2004;40:1387-1395.
9. Argo CK, Caldwell SH. Epidemiology and natural history of nonalcoholic steatohepatitis. Clin Liver Dis 2009;13:511-531.
10. Gramlich T, Kleiner DE, McCullough AJ, Matteoni CA, Boparai N, Younossi ZM. Pathologic features associated with fibrosis in nonalcoholic fatty liver disease. Hum Pathol 2004;35:196-199.
11. Matteoni CA, Younossi ZM, Gramlich T, Boparai N, Liu YC, McCullough AJ. Nonalcoholic fatty liver disease: a spectrum of clinical and pathological severity. Gastroenterology 1999;116:1413-1419.
12. Angulo P, Keach JC, Batts KP, Lindor KD. Independent predictors of liver fibrosis in patients with nonalcoholic steatohepatitis. Hepatology 1999;30:1356-1362.
13. McCullough AJ. The epidemiology and risk factors of NASH. In: Farrell GC, George J, Hall PdaM, McCullough AJ, eds. Fatty Liver Disease. NASH and Related Disorders. Malden, MA: Blackwell; 2005:23-37.
14. Ekstedt M, Franzén LE, Mathiesen UL, Thorelius L, Holmqvist M, Bodemar G, Kechagias S. Long-term follow-up of patients with NAFLD and elevated liver enzymes. Hepatology 2006;44:865-873.
15. Rubinstein E, Lavine JE, Schwimmer JB. Hepatic, cardiovascular, and endocrine outcomes of the histological subphenotypes of nonalcoholic fatty liver disease. Semin Liver Dis 2008;28:380-385.
16. Guzman G, Brunt EM, Petrovic LM, Chejfec G, Layden TJ, Cotler SJ. Does nonalcoholic fatty liver disease predispose patients to hepatocellular carcinoma in the absence of cirrhosis? Arch Pathol Lab Med 2008; 132:1761-1766.

17. Sanyal AJ, Banas C, Sargeant C, Luketic VA, Sterling RK, Stravitz RT, et al. Similarities and differences in outcomes of cirrhosis due to nonalcoholic steatohepatitis and hepatitis C. Hepatology 2006;43:682-689.
18. Adams LA, Lymp JF, St Sauver J, Sanderson SO, Lindor KD, Feldstein A, Angulo P. The natural history of nonalcoholic fatty liver disease: a population-based cohort study. Gastroenterology 2005;129:113-121.
19. Adams LA, Sanderson S, Lindor KD, Angulo P. The histological course of nonalcoholic fatty liver disease: a longitudinal study of 103 patients with sequential liver biopsies. J Hepatol 2005;42:132-138.
20. Angulo P. Nonalcoholic fatty liver disease. N Engl J Med 2002;346: 1221-1231.
21. Rockey DC, Caldwell SH, Goodman ZD, Nelson RC, Smith AD. Liver biopsy: AASLD position paper. Hepatology 2009;49:1017-1044.
22. Cusi K, Chang Z, Harrison S, Lomonaco R, Bril F, Orsak B, et al. Limited value of plasma cytokeratin-18 as a biomarker for NASH and fibrosis in patients with nonalcoholic fatty liver disease (NAFLD). J Hepatol 2014;60:167-174.
23. Angulo P, Hui JM, Marchesini G, Bugianesi E, George J, Farrell GC, et al. The NAFLD fibrosis score: a noninvasive system that identifies liver fibrosis in patients with NAFLD. Hepatology 2007;45:846-854.
24. Guha IN, Parkes J, Roderick P, Chattopadhyay D, Cross R, Harris S, et al. Noninvasive markers of fibrosis in nonalcoholic fatty liver disease: validating the European Liver Fibrosis Panel and exploring simple markers. Hepatology 2008;47:455-460.
25. Shah AG, Lydecker A, Murray K, Tetri BN, Contos MJ, Sanyal AJ; Nash Clinical Research Network. Comparison of noninvasive markers of fibrosis in patients with nonalcoholic fatty liver disease. Clin Gastroenterol Hepatol 2009;7:1104-1112.
26. Friedrich-Rust M, Nierhoff J, Lupsor M, Sporea I, Fierbinteanu-Braticevici C, Strobel D, et al. Performance of acoustic radiation force impulse imaging for the staging of liver fibrosis: a pooled meta-analysis. J Viral Hepat 2012;19:e212-e219.
27. Myers RP, Pomier-Layrargues G, Kirsch R, Pollett A, Duarte-Rojo A, Wong D, et al. Feasibility and diagnostic performance of the FibroScan XL probe for liver stiffness measurement in overweight and obese patients. Hepatology 2012;55:199-208.
28. Palmeri ML, Wang MH, Rouze NC, Abdelmalek MF, Guy CD, Moser B, et al. Noninvasive evaluation of hepatic fibrosis using acoustic radiation force-based shear stiffness in patients with nonalcoholic fatty liver disease. J Hepatol 2011;55:666-672.
29. Wong VW, Vergniol J, Wong GL, Foucher J, Chan AW, Chermak F, et al. Liver stiffness measurement using XL probe in patients with nonalcoholic fatty liver disease. Am J Gastroenterol 2012;107:1862-1871.
30. Kim D, Kim WR, Talwalkar JA, Kim HJ, Ehman RL. Advanced fibrosis in nonalcoholic fatty liver disease: noninvasive assessment with MR elastography. Radiology 2013;268:411-419.
31. Noureddin M, Lam J, Peterson MR, Middleton M, Hamilton G, Le TA, et al. Utility of magnetic resonance imaging versus histology for quantifying changes in liver fat in nonalcoholic fatty liver disease trials. Hepatology 2013;58:1930-1940.
32. Le TA, Chen J, Changchien C, Peterson MR, Kono Y, Patton H, et al.; San Diego Integrated NAFLD Research Consortium (SINC). Effect of colesevelam on liver fat quantified by magnetic resonance in nonalcoholic steatohepatitis: a randomized controlled trial. Hepatology 2012;56:922-932.
33. Permutt Z, Le TA, Peterson MR, Seki E, Brenner DA, Sirlin C, Loomba R. Correlation between liver histology and novel magnetic resonance imaging in adult patients with non-alcoholic fatty liver disease—MRI accurately quantifies hepatic steatosis in NAFLD. Aliment Pharmacol Ther 2012;36:22-29.
34. Kleiner DE, Brunt EM, Van Natta M, Behling C, Contos MJ, Cummings OW, et al.; Nonalcoholic Steatohepatitis Clinical Research Network. Design and validation of a histological scoring system for nonalcoholic fatty liver disease. Hepatology 2005;41:1313-1321.
35. Yin M, Talwalkar JA, Glaser KJ, Manduca A, Grimm RC, Rossman PJ, et al. Assessment of hepatic fibrosis with magnetic resonance elastography. Clin Gastroenterol Hepatol 2007;5:1207-1213.e2.
36. Chen J, Talwalkar JA, Yin M, Glaser KJ, Sanderson SO, Ehman RL. Early detection of nonalcoholic steatohepatitis in patients with nonalcoholic fatty liver disease by using MR elastography. Radiology 2011;259:749-756.
37. Kim D, Kim WR, Talwalkar JA, Kim HJ, Ehman RJ. Advanced fibrosis in nonalcoholic fatty liver disease: noninvasive assessment with MR elastography. Radiology 2013;268:411-419.
38. Venkatesh SK, Yin M, Ehman RL. Magnetic resonance elastography of liver: technique, analysis, and clinical applications. J Magn Reson Imaging 2013;37:544-555.
39. Tang A, Tan J, Sun M, Hamilton G, Bydder M, Wolfson T, et al. Nonalcoholic fatty liver disease: MR imaging of liver proton density fat fraction to assess hepatic steatosis. Radiology 2013;267:422-431.
40. Yokoo T, Shiehmorteza M, Hamilton G, Wolfson T, Schroeder ME, Middleton MS, et al. Estimation of hepatic proton-density fat fraction by using MR imaging at 3.0 T. Radiology 2011;258:749-759.
41. Yokoo T, Bydder M, Hamilton G, Middleton MS, Gamst AC, Wolfson T, et al. Nonalcoholic fatty liver disease: diagnostic and fat-grading accuracy of low-flip-angle multiecho gradient-recalled-echo MR imaging at 1.5 T. Radiology 2009;251:67-76.
42. Reeder SB, Hu HH, Sirlin CB. Proton density fat-fraction: a standardized MR-based biomarker of tissue fat concentration. J Magn Reson Imaging 2012;36:1011-1014.
43. Reeder SB, Cruite I, Hamilton G, Sirlin CB. Quantitative assessment of liver fat with magnetic resonance imaging and spectroscopy. J Magn Reson Imaging 2011;34:729-749.
44. Bydder M, Yokoo T, Hamilton G, Middleton MS, Chavez AD, Schwimmer JB, et al. Relaxation effects in the quantification of fat using gradient echo imaging. Magn Reson Imaging 2008;26:347-359.
45. Bydder M, Shiehmorteza M, Yokoo T, Sugay S, Middleton MS, Girard O, et al. Assessment of liver fat quantification in the presence of iron. Magn Reson Imaging 2010;28:767-776.
46. Liu CY, McKenzie CA, Yu H, Brittain JH, Reeder SB. Fat quantification with IDEAL gradient echo imaging: correction of bias from T(1) and noise. Magn Reson Med 2007;58:354-364.
47. Reeder SB, Robson PM, Yu H, Shimakawa A, Hines CD, McKenzie CA, Brittain JH. Quantification of hepatic steatosis with MRI: the effects of accurate fat spectral modeling. J Magn Reson Imaging 2009;29:1332-1339.
48. Hamilton G, Yokoo T, Bydder M, Cruite I, Schroeder ME, Sirlin CB, Middleton MS. In vivo characterization of the liver fat (1)H MR spectrum. NMR Biomed 2011;24:784-790.
49. Hansen KH, Schroeder ME, Hamilton G, Cirlin CB, Bydder M. Robustness of fat quantification using chemical shift imaging. Magn Reson Imaging 2012;30:151-157.
50. Kang GH, Cruite I, Shiehmorteza M, Wolfson T, Gamst AC, Hamilton G, et al. Reproducibility of MRI-determined proton density fat fraction across two different MR scanner platforms. J Magn Reson Imaging 2011;34:928-934.
51. Bonekamp S, Tang A, Mashhood A, Wolfson T, Changchien C, Middleton MS, et al. Spatial distribution of MRI-determined hepatic proton density fat fraction in adults with nonalcoholic fatty liver disease. J Magn Reson Imaging 2014;39:1525-1532.
52. Xanthakos SA, Podberesky DJ, Serai SD, Miles L, King EC, Balistreri WF, et al. Use of magnetic resonance elastography to assess hepatic fibrosis in children with chronic liver disease. J Pediatr 2014;164:186-188.
53. Castera L, Vilgrain V, Angulo P. Noninvasive evaluation of NAFLD. Nat Rev Gastroenterol Hepatol 2013;10:666-675.
54. Berzigotti A, Castera L. Update on ultrasound imaging of liver fibrosis. J Hepatol 2013;59:180-182.
55. Noureddin M, Loomba R. Nonalcoholic fatty liver disease: Indications for liver biopsy and noninvasive biomarkers. Clin Liver Dis 2012;1:103-106.
56. Asrani SK, Talwalkar JA, Kamath PS, Shah VH, Saracino G, Jennings L, et al. Role of magnetic resonance elastography in compensated and decompensated liver disease. J Hepatol 2014;60:934-939.

Supporting Information

Additional Supporting Information may be found at onlinelibrary.wiley.com/doi/10.1002/hep.27362/suppinfo.